Bioorganic & Medicinal Chemistry Letters 30 (2020) 127529

Contents lists available at ScienceDirect

Bioorganic & Medicinal Chemistry Letters

journal homepage: www.elsevier.com/locate/bmcl

Synthesis and SAR of a series of $mGlu_7$ NAMs based on an ethyl-8-methoxy-4-(4-phenylpiperazin-1-yl)quinoline carboxylate core

Jacob J. Kalbfleisch[a,c], Carson W. Reed[a,b], Charlotte Park[a,b], Paul K. Spearing[a,b], Marc C. Quitalig[a,b], Matthew T. Jenkins[a,b], Alice L. Rodriguez[a,b], Anna L. Blobaum[a,b], P. Jeffrey Conn[a,b,d,e], Colleen M. Niswender[a,b,d,e,*], Craig W. Lindsley[a,b,c,e,*]

[a] Warren Center for Neuroscience Drug Discovery, Vanderbilt University, Nashville, TN 37232, USA
[b] Department of Pharmacology, Vanderbilt University School of Medicine, Nashville, TN 37232, USA
[c] Department of Chemistry, Vanderbilt University, Nashville, TN 37232, USA
[d] Vanderbilt Kennedy Center, Vanderbilt University Medical Center, Nashville, TN 37232, USA
[e] Vanderbilt Institute of Chemical Biology, Vanderbilt University, Nashville, TN 37232, USA

ARTICLE INFO

Keywords:
$mGlu_7$
Metabotropic glutamate receptor
Negative Allosteric modulator (NAM)
Structure-activity-relationship (SAR)

ABSTRACT

A High-Throughput Screening (HTS) campaign identified a fundamentally new $mGlu_7$ NAM chemotype, based on an ethyl-8-methoxy-4-(4-phenylpiperazin-1-yl)quinolone carboxylate core. The initial hit, VU0226390, was a potent $mGlu_7$ NAM (IC_{50} = 647 nM, 6% L-AP4 min) with selectivity versus the other group III mGlu receptors (> 30 μM vs. $mGlu_4$ and $mGlu_8$). A multi-dimensional optimization effort surveyed all regions of this new chemotype, and found very steep SAR, reminiscent of allosteric modulators, and unexpected piperazine mimetics (whereas classical bioisosteres failed). While $mGlu_7$ NAM potency could be improved (IC_{50}s ~ 350 nM), the necessity of the ethyl ester moiety and poor physiochemical and DMPK properties precluded optimization towards *in vivo* tool compounds or clinical candidates. Still, this hit-to-lead campaign afforded key medicinal chemistry insights and new opportunities.

Recently, metabotropic glutamate receptor subtype 7 ($mGlu_7$) has garnered great interest as a viable target for a broad range of CNS disorders (e.g., PTSD, schizophrenia, depression, epilepsy, ADHD) and neurodevelopmental disorders (e.g., Rett syndrome and autism).[1–15] Compared to other mGlu receptors, $mGlu_7$ is one of the least explored and there is limited validation of its therapeutic potential due to a lack of selective, small molecule probes.[16,17] To study $mGlu_7$ activation, the field has no selective $mGlu_7$ positive allosteric modulators (PAMs), but must instead rely on $mGlu_7$-preferring PAMs or *pan*-Group III PAMs in combination with selective negative allosteric modulators (NAMs) to isolate $mGlu_7$ activity.[18] NAMs are more advanced, with essentially four distinct chemotypes (**1**/**2**, **3**, **4**, **5**–**7**, Fig. 1) of subtype selective ligands; however, first generation NAMs were electrophilic and suffered from poor disposition.[19–24] Recently new CNS-penetrant $mGlu_7$ NAMs, suitable as *in vivo* tool compounds (e.g. **6** and **7**) have become available.[25–27]

Based on the pharmacological intricacies of allosteric modulators, we prefer to have multiple chemotypes to probe each mode of pharmacology. Here, we report on the discovery of a fundamentally new $mGlu_7$ NAM chemotype, based on an ethyl-8-methoxy-4-(4-phenylpiperazin-1-yl)quinolone carboxylate core, derived from a functional HTS campaign. While SAR was steep, $mGlu_7$ potency could be improved, and key medicinal chemistry insights were gained with respect to non-obvious bioisosteres.

The structure of VU0226390 (**8**), based on an ethyl-8-methoxy-4-(4-phenylpiperazin-1-yl)quinolone carboxylate core, and the corresponding multi-dimensional optimization plan is depicted in Fig. 2. VU0226390 (**8**) was an attractive hit for several reasons: 1) it was a novel chemotype with selective sub-micromolar potency ($mGlu_7$ IC_{50} = 647 nM, 6% L-AP_4 min, > 30 μM vs. $mGlu_4$ and $mGlu_8$), an acceptable DMPK profile (f_u (r,h) = 0.016, 0.018, CL_{hep} = 60 mL/min/kg) and opportunities for a straightforward, modular synthetic plan. However, the ester moiety was a drawback as a potential metabolic liability, as was the inherent DMAP-like core structure of the piperazinyl quinoline. Thus, the optimization plan was to find replacements for these two concerning features, while also exploring alternatives for the distal 2-OMe phenyl ring and the 8-OMe quinolone core.

The synthetic route shown in Scheme 1, and variations thereof, was employed to access analogs **11**, surveying multiple dimensions of the hit **8**. Aniline **9** was heated with diethyl ethoxymethylenemalonate, in

* Corresponding authors at: Warren Center for Neuroscience Drug Discovery, Vanderbilt University, Nashville, TN 37232, USA.
E-mail addresses: colleen.niswender@vanderbilt.edu (C.M. Niswender), craig.lindsley@vanderbilt.edu (C.W. Lindsley).

https://doi.org/10.1016/j.bmcl.2020.127529
Received 8 June 2020; Received in revised form 24 August 2020; Accepted 27 August 2020
Available online 02 September 2020
0960-894X/

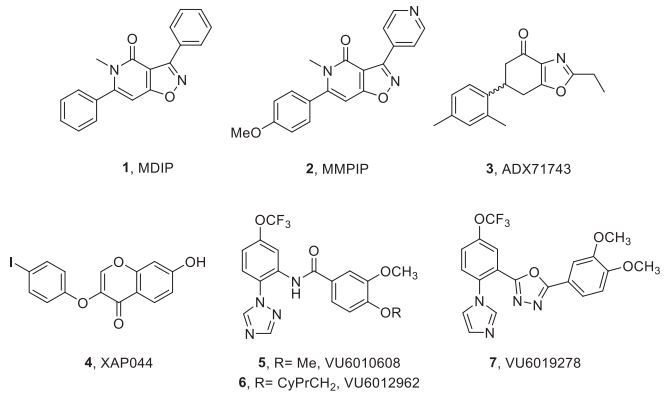

Fig. 1. Structures of reported $mGlu_7$ NAMs **1–7**, note the limited chemical diversity. NAMs **6** and **7** are robust, CNS penetrant *in vivo* tool compounds.

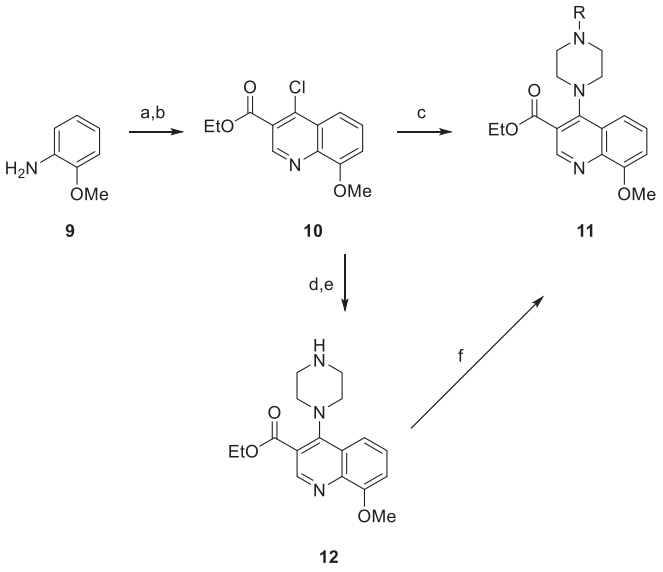

Scheme 1. Synthesis of analogs **11** of the $mGlu_7$ NAM hit **8**[a]. [a]*Reagents and conditions*: (a) DEEMM, 140 °C, neat, 45 min, then Ph_2O, 250 °C, 30 min, 31%; (b) $POCl_3$, neat, 100 °C, 20 min, 78%; (c) aryl/heteroaryl piperazine, DIEA, DMF, 60 °C, 4 h, 7–66%; (d) *N*-Boc-piperazine, DIEA, DMF, 60 °C, 4 h, 74%; (e) 1:1 TFA:DCM, rt, 1 h, 98%; (f) Ar/Het-Br (I), Pd_2dba_3, P^tBu_3, NaO^tBu, toluene, mw, 115 °C, 1 h, 4–60%.

the absence of solvent to provide enamines, which were suspended in diphenyl ether and heated to 250 °C to promote cyclization to the corresponding quinolone in 31% yield. Standard conversion to the 4-chloroquinoline **10** proceeded under $POCl_3$ conditions in 78% yield. S_NAr with various aryl/heteroaryl piperazines afforded analogs **11** in yields ranging from 7 to 66%. Alternatively, *N*-Boc-piperazine could be employed in the S_NAr step, such that after deprotection, e.g. **12**, a wide range of aryl/heteroaryl moieties could be installed via Buchwald-Hartwig couplings to also access analogs **11** in good overall yields. The SAR for analogs **11** proved interesting.

The ethyl ester moiety of **8** emerged as a necessary pharmacophore for $mGlu_7$ NAM activity, and proved stable under our cell-based assay conditions. Replacement with a methyl ester lost ~6-fold in activity (IC_{50} = 4 μM), but this was likely due to hydrolysis (the methyl ester partially hydrolyzed in cell buffer) to the corresponding acid, which was inactive (IC_{50} > 30 μM). Similarly, the primary carboxamide congener, as well as diverse secondary and tertiary amides, all proved devoid of $mGlu_7$ NAM activity. Small alkyl, cycloalkyl and ether replacements for the ethyl ester were uniformly inactive. Thus, we elected to hold the ethyl ester constant, optimize activity elsewhere, and then return to find a more suitable replacement.

We surveyed a diverse array of substituted aryl and heteroaryl moieties to replace the 2-OMe phenyl moiety in **8** (Table 1) in an attempt to improve $mGlu_7$ NAM potency and/or disposition with analogs **11**. SAR was steep, with substitution only tolerated in the 2-position on the distal phenyl ring, e.g., 3-OMe and 4-OMe phenyl congeners were inactive. Ethers in the 2-position larger than methyl (**11a-c**) lost activity, as did 2-Cl (**11d**), 2-Me (**11e**), 2-CN (**11f**) and 2-F (**11h**) substitutions. From this survey, only the 2-SMePh derivative (**11g**) displayed improved potency (IC_{50} = 510 nM) over **8**, with a slight improvement in rat predicted hepatic clearance (CL_{hep} = 51.3 mL/min/kg). However, the corresponding sulfoxide and sulfone of **11g** proved devoid of $mGlu_7$ NAM activity. While di-OMe substituted analogs, such as **11i** and **11j**, retained $mGlu_7$ NAM potency, their disposition (as expected) was inferior to **8**. Direct heterocyclic congeners of **8**, such as the pyridine **11l** or pyrazine **11m** displayed modest potency. However, all 5-membered heterocyclic anlaogs (**11n-p**) proved inactive.

In parallel, we evaluated replacements for the quinolone core of **8** (Fig. 3). Truncation to a monocyclic pyridine, **13a**, resulted in a ~6.5-fold loss of potency, as did both regioisomeric thienopyridines **13b** and **13c**, highlighting the lack of bioisosterism with these substitutions.

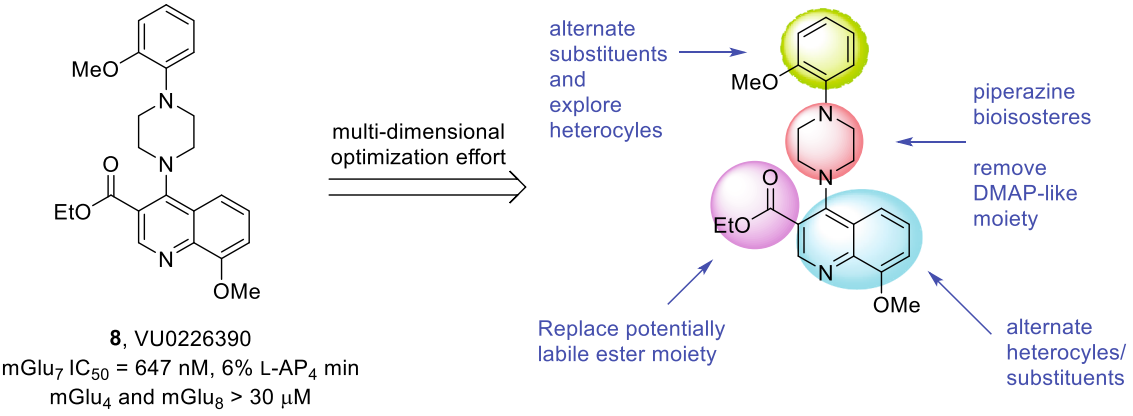

Fig. 2. Multi-dimensional optimization plan for the $mGlu_7$ NAM hit **8**, VU0226390.

Table 1

Structure and $mGlu_7$ NAM activities of analogs **11**.

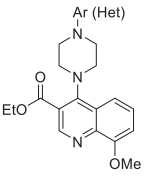

11

Cmpd	Ar/Het	$mGlu_7$ IC_{50} (μM)[a]	$mGlu_7$ % L-AP_4 Min
8	2-OMePh	0.65	5.6
11a	2-OEtPh	5.1	8.7
11b	2-O^{i}PrPh	2.3	6.5
11c	2-OCF_3Ph	> 30	–
11d	2-ClPh	> 30	–
11e	2-MePh	> 10	41
11f	2-CNPh	4.2	14
11g	2-SMePh	0.51	4.7
11h	2-FPh	6.1	12
11i	2,4-diOMePh	1.9	9.0
11j	2,6-diOMePh	0.80	11
11k	2-OMe-5-FPh	2.1	15
11l		1.5	10
11m		3.0	11
11n		> 30	–
11o		> 30	–
11p		> 30	–

[a]For SAR determination, calcium mobilization assays with rat $mGlu_7/G_{\alpha 15}$/HEK cells were performed in the presence of a fixed EC_{80} concentration of L-AP_4; values represent (n = 1) independent experiments performed in triplicate.[25]

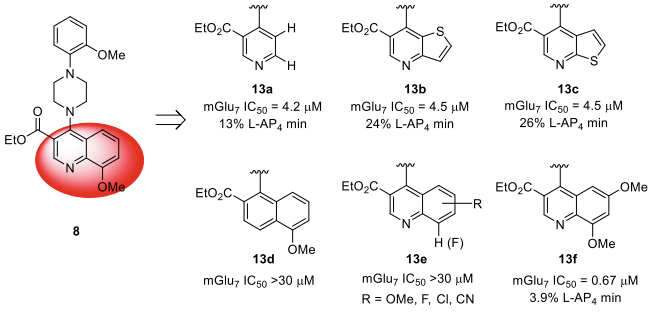

Fig. 3. SAR efforts to replace the quinolone core of $mGlu_7$ NAM **8**.

Replacement with a naphthalene (**13d**) proved inactive, as did replacement of the 8-OMe moiety with either a hydrogen or fluoride atom (**13e**). Here, only a 6,8-diOMe congener, **13f**, proved equipotent to **8**, but once again displayed a poor disposition profile. Thus, moving forward, we would maintain the 8-OMe quinolone core and the 2-OMe phenyl moiety of **8** as we surveyed the piperazine linker (Table 2).

SAR around the piperazine core of **8** (Table 2), with analogs **13**, proved interesting. The addition of a racemic methyl group to either the 3-position (**14a**) or the 2-position (**14b**), led to an ~2-fold loss in $mGlu_7$ NAM potency. Cleavage of the piperazine ring, as in **14c**, lost ~6-fold, while deletion of the proximal piperazine nitrogen proved inactive.

Table 2

Structure and $mGlu_7$ NAM activities of analogs **14**.

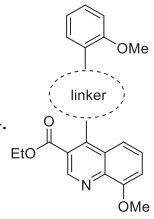

13

Cmpd	Linker	$mGlu_7$ IC_{50} (μM)[a]	$mGlu_7$ % L-AP_4 Min
8	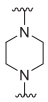	0.65	5.6
14a	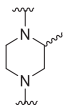	1.3	8.6
14b	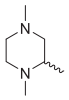	1.5	6.1
14c	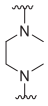	4.4	9.6
14d	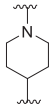	> 10	41
14e	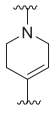	3.6	9.6
14f	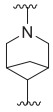	> 30	–
14g	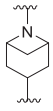	> 10	41
14h	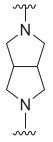	> 10	57
14i		> 30	–
14j	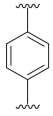	2.9	4.2

[a]For SAR determination, calcium mobilization assays with rat $mGlu_7/G_{\alpha 15}$/HEK cells were performed in the presence of a fixed EC_{80} concentration of glutamate; values represent (n = 1) independent experiments performed in triplicate.[25]

Incorporating unsaturation, as with **14e**, regained potency ($mGlu_7$ IC_{50} = 3.5 μM), while cyclic constraints, e.g, **14f** and **14 g**, proved inactive. Classical piperazine bioisosteres, such as [3.3.0] system (**14 h**)

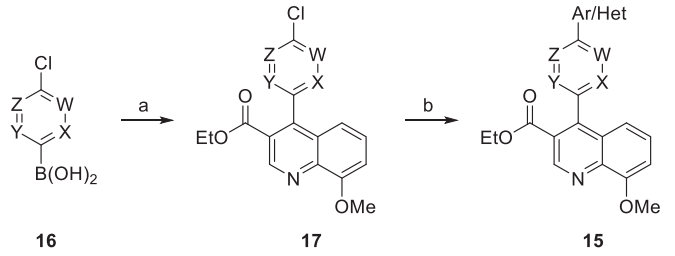

16 17 15

Scheme 2. Synthesis of heteroaryl linker analogs **15**[a]. [a]Reagents and conditions: (a) **10**, 10 mol% Pd(dppf)Cl_2, Cs_2CO_3, 4:1 dioxane:water, mw, 110 °C, 30 min, 45–57%; (b) Ar/Het-B(OH)$_2$, 10 mol% Pd(dppf)Cl_2, Cs_2CO_3, 4:1 dioxane:water, mw, 110 °C, 30 min, 25–69%.

and the spiroazetidine (**14i**), were not productive in this context. Surprisingly, a biphenyl monomer we had 'in house' proved intriguing and demonstrated that a simple phenyl ring (**14j**) could replace the piperazine linker with reasonable potency (IC_{50} = 2.9 μM). However, the DMPK profile of **14j** was poor (f_u (r, h) < 0.001, CL_{hep} (rat) = 66 mL/min/kg), leading the team to consider replacement of the phenyl ring with polar/basic heterocycles, e.g., analogs **15**. Analogs **15** were readily prepared according to Scheme 2. Utilizing commercial heteroaryl chloro-boronic acids **16**, in a chemoselective Suzuki coupling with intermediate **10**, provided derivatives **17** in yields ranging from 45 to 57%. A second Suzuki coupling with aryl boronic acids delivered final compounds **15** in good overall yields. As shown in Table 3, SAR within this sub-series was more robust than in the preceding saturated systems. Replacement of the phenyl linker with a 6-pyridyl congener, **15a**, proved to be equipotent (IC_{50} = 2.8 μM), but the 5-pyridyl regioisomer, **15b**, was a potent and efficacious $mGlu_7$ NAM (IC_{50} = 0.60 μM, 6.5% L-AP_4 min). A slight increase in potency (IC_{50} = 0.37 μM, 6.3% L-AP_4 min and IC_{50} = 0.41 μM, 5.6% L-AP_4 min) was noted with both the 2-OEtPh analog (**15c**) and the 2-SMePh derivative (**15d**), respectively. A pyrimidine congener lost (**15f**) activity (IC_{50} = 2.4 μM, 12.0% L-AP_4 min) while a pyrazine maintained good $mGlu_7$ NAM activity (IC_{50} = 0.54 μM, 5.1% L-AP_4 min). The addition of a pendant methoxy moiety to the pyridine ring of **15b**, affording **15 h**, led to a more potent $mGlu_7$ NAM (IC_{50} = 0.35 μM, 3.6% L-AP_4 min). Even 5-membered heterocycles, such as pyrrole **15j,** was a competent surrogate for the phenyl linker. Finally, as with **13f**, the incorporation of an additional methoxy group in the 6-position of the quinoline ring system, e.g., **18** and **19** (Fig. 4), led to sub-micromolar $mGlu_7$ NAMs.

While none of these new $mGlu_7$ NAMs possessed *in vitro* or *in vivo* DMPK profiles (e.g, **15h**, low fraction unbound: f_u (rat, mouse) = 0.01, 0.01, BHB f_u (rat, mouse) = 0.04, 0.04, high predicted hepatic clearance (CL_{hep} (rat, mouse) = 65.2 and 66.1 mL.mkin/kg) and high clearance *in vivo*, CL_p = 70 mL/min/kg) worthy of advancement as *in vivo* tools, they are unique *in vitro* pharmacological tools with selectivity against the other mGlu receptors. Upon closer inspection of analogs **15**, these resemble classical terphenyl α-helical mimetic protein–protein inhibitor (PPI) chemotype **20** (Fig. 5), with clear overlap of the prototypical i, i + 3/4 and i + 7 moieties in **15h**.[28,29] As **15h** is structurally distinct from previously reported $mGlu_7$ NAMs, and due to the resemblance to α-helical mimetic protein–protein inhibitor (PPI) chemotypes, the exciting prospect exists that this family of NAMs has a unique mode of pharmacological inhibition of $mGlu_7$.

In summary, we have reported on the multi-dimensional optimization of a fundamentally new $mGlu_7$ NAM chemotype, based on an ethyl-8-methoxy-4-(4-phenylpiperazin-1-yl)quinolone carboxylate core; moreover, we found that aromatic heterocycles, such as pyridines, are an unlikely bioisostere for the central piperazine motif. SAR led to the discovery of a unique terphenyl chemotype, reminiscent of α-helical mimetic PPIs-, a first in the mGlu allosteric ligand world. Studies are underway to evaluate the mechanism of inhibition of $mGlu_7$ by **15h** in comparison to chemically distinct $mGlu_7$ NAM **6**. These more laborious studies are underway and will be reported in due course.

Table 3

Structure and $mGlu_7$ NAM activities of analogs **15**.

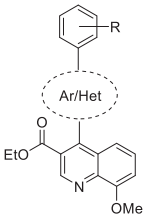

15

Cmpd	Ar/Het	R	$mGlu_7$ IC_{50} (μM)[a]	$mGlu_7$ % L-AP_4 Min
15a	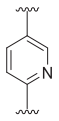	2-OMe	2.8	6.8
15b	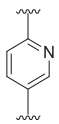	2-OMe	0.60	6.5
15c	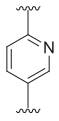	2-OEt	0.37	6.3
15d	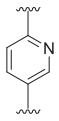	2-SMe	0.41	5.6
15e	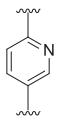	2-O^{i}Pr	1.5	5.8
15f	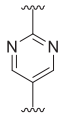	2-OMe	2.4	12
15 g	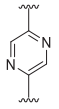	2-OMe	0.54	5.1
15 h	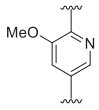	2-OMe	0.35	3.6
15i	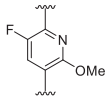	2-OMe	2.1	24
15j	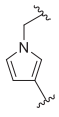	2-OMe	1.2	6.5

[a]For SAR determination, calcium mobilization assays with rat $mGlu_7/G_{\alpha 15}$/HEK cells were performed in the presence of a fixed EC_{80} concentration of glutamate; values represent (n = 1) independent experiments performed in triplicate.[25]

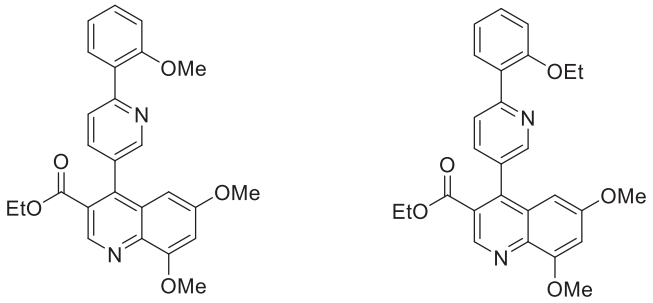

18

$mGlu_7$ IC_{50} = 0.88 μM
3.5% L-AP_4 min

19

$mGlu_7$ IC_{50} = 0.81 μM
5.0% L-AP_4 min

Fig. 4. 6,8-DiOMe substituted terphenyl $mGlu_7$ NAMs **18** and **19**.

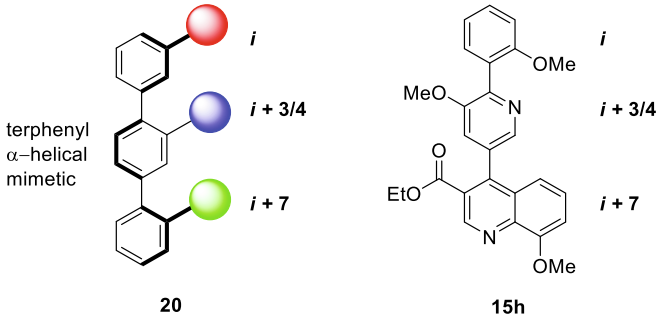

20 **15h**

Fig. 5. The classical terphenyl α-helical mimetic PPI chemotype **20**, and the close overlay with terphenyl-based $mGlu_7$ NAMs, such as **15h**.

Declaration of Competing Interest

The authors declare that they have no known competing financial interests or personal relationships that could have appeared to influence the work reported in this paper.

Acknowledgments

We thank the Warren Family and Foundation for establishing the William K. Warren, Jr. Chair in Medicine (C.W.L.) and endowing the Warren Center for Neuroscience Drug Discovery. The authors also acknowledge funding by CDMRP Grant W81XWH-17-1-0266 and MH104158 (to C.M.N.).

References

1. Fisher NM, Seto M, Lindsley CW, et al. *Front Mol Neurosci.* 2018;11.
2. Sansig G, Bushell TJ, Clarke VR, et al. *J Neurosci.* 2001;21:8734.
3. Goddyn H, Callaerts-Vegh Z, Stroobants S, et al. *Neurobiol Learn Mem.* 2008;90:103.
4. Palucha A, Klak K, Branski P, et al. *Psychopharmacology.* 2007;194:555.
5. Callaerts-Vegh Z, Beckers T, Ball SM, et al. *J Neurosci.* 2006;26:6573.
6. Mitsukawa K, Mombereau C, Lötscher E, et al. Neuropsychopharmacology 31 (2006) 1112.
7. Hölscher C, Schmid S, Pilz PK, et al. *Learn. Mem.* 2005;12:450.
8. Hölscher C, Schmid S, Pilz PK, et al. *Behav Brain Res.* 2004;154:473.
9. Bushell TJ, Sansig G, Collett VJ, et al. *ScientificWorldJournal.* 2002;2:730.
10. Masugi M, Yokoi M, Shigemoto R, et al. *J Neurosci.* 1999;19:955.
11. Fisher NM, Gogliotti RG, Vermudez SAD, et al. *ACS Chem Neurosci.* 2018;9:2210.
12. Gogliotti RG, Senter RK, Fisher NM, et al. Sci Trans Med 9 (2017) eaai7459.
13. Jalan-Sakrikar N, Field JR, Klar R, et al. *ACS Chem Neurosci.* 2014;5:1221.
14. Tassin V, Girard B, Chotte A, et al. *Front Neural Circuits.* 2016;10:article 10.
15. Girard B, Tuduri P, Moreno MP, et al. *Neurobiol Dis.* 2019;129:13.
16. Niswender CM, Conn PJ. *Ann Rev Pharmacol Toxicol.* 2010;50:295.
17. Lindsley CW, Emmitte KA, Hopkins CR, et al. *Chem Rev.* 2016;116:6707.
18. Abe M, Seto M, Gogliotti RG, et al. *ACS Med Chem Lett.* 2017;8:1110.
19. Suzuki G, Tsukamoto N, Fushiki H, et al. *J Pharmacol Exp Ther.* 2007;232:147.
20. Nakamura M, Kurihara H, Suzuki G, et al. *Bioorg Med Chem Lett.* 2010;20:726.
21. Kalinichev M, Rouillier M, Girard F, et al. *J Pharmacol Exp Ther.* 2013;344:624.
22. Gee CE, Peterlik D, Neuhäuser C. *J Biol Chem.* 2014;289:10975.
23. Niswender CM, Johnson KA, Miller NR, et al. *Mol Pharmacol.* 2010;77(77):459.
24. Reed CW, McGowan KM, P.K. et al. ACS Med Chem Lett 8 (2017) 1326.
25. Reed CW, Yohn SE, Washecheck JP, et al. *J Med Chem.* 2019;62:1690.
26. Reed CW, Washecheck JP, Quitalig MC, et al. *Bioorg Med Chem Lett.* 2019;29:1211.
27. Vázquez-Villa H, Trabanco AA. *MedChemComm.* 2019;10:193.
28. Jayatunga MKP, Thompson S, Hamilton AD. *Bioorg Med Chem Lett.* 2014;24:717.
29. Antuch W, Menon S, Chen Q-Z, et al. Bioorg Med Chem Lett 16 (2006) 1740.